

Centre for Archaeology Report 7/2002

Michelmersh, Hampshire: Archaeomagnetic Dating Report 2002

Paul Linford

© English Heritage 2002

ISSN 1473-9224

The Centre for Archaeology Reports Series incorporates the former Ancient Monuments Laboratory Report Series. Copies of Ancient Monuments Laboratory Reports will continue to be available from the Centre for Archaeology (see back of cover for details).

Michelmersh, Hampshire: Archaeomagnetic Dating Report 2002

Paul Linford

Summary

During excavations by Wessex Archaeology in advance of the laying of a new pipeline by Southern Water at Michelmersh near Romsey in Hampshire, an Anglo-Saxon clamp kiln was discovered. Unusually for such a feature, complete pots were found *in-situ*, which, for unknown reasons, had been fired but never recovered by the operators of the kiln. Providing a date for the last firing of the kiln was of potentially major significance for the regional Anglo-Saxon pottery chronology, so the Centre for Archaeology were asked to provide archaeomagnetic analysis of the feature. From this analysis it was possible to date the last use of the kiln to the end of the 10th century AD which was in good agreement with the date estimated from the existing pottery chronology for the area.

Keywords

Archaeomagnetism

Author's address

Centre for Archaeology, Fort Cumberland, Fort Cumberland Road, Eastney, Portsmouth, PO4 9LD

Many CfA reports are interim reports which make available the results of specialist investigations in advance of full publication. They are not subject to external refereeing, and their conclusions may sometimes have to be modified in the light of archaeological information that was not available at the time of the investigation. Readers are therefore advised to consult the author before citing the report in any publication and to consult the final excavation report when available.

Opinions expressed in CfA reports are those of the author and are not necessarily those of English Heritage.

**MICHELMERSH, Hampshire:
Archaeomagnetic Dating Report 2002**

Introduction

During excavations by Wessex Archaeology in advance of the laying of a new pipeline by Southern Water at Michelmersh near Romsey in Hampshire, an Anglo-Saxon clamp kiln was discovered (SU 344 264, Longitude 1.5°W, Latitude 51.0°N). The kiln consisted of a hole of about 1m by 0.7m in plan and about 0.3m deep cut into the natural sandy clay soil and lined with rammed chalk pieces. Unusually for such a feature, complete pots were found *in-situ* (Figure 1, right), which for unknown reasons had been fired but never recovered by the operators of the kiln. Consultations between Mike Allen of Wessex Archaeology, Rob Perrin, the EH inspector of Ancient Monuments for Hampshire, and Sarah Jennings, the CfA's post medieval pottery expert, determined that obtaining a date for the last firing of the kiln would provide a major contribution to regional pottery chronology for the Anglo-Saxon period. Hence, the Centre for Archaeology were asked to provide archaeomagnetic analysis of the feature.

The feature was sampled for archaeomagnetic analysis by Louise Martin and the author on the 1st of November 2001. Subsequent measurement and evaluation was also performed by the author.

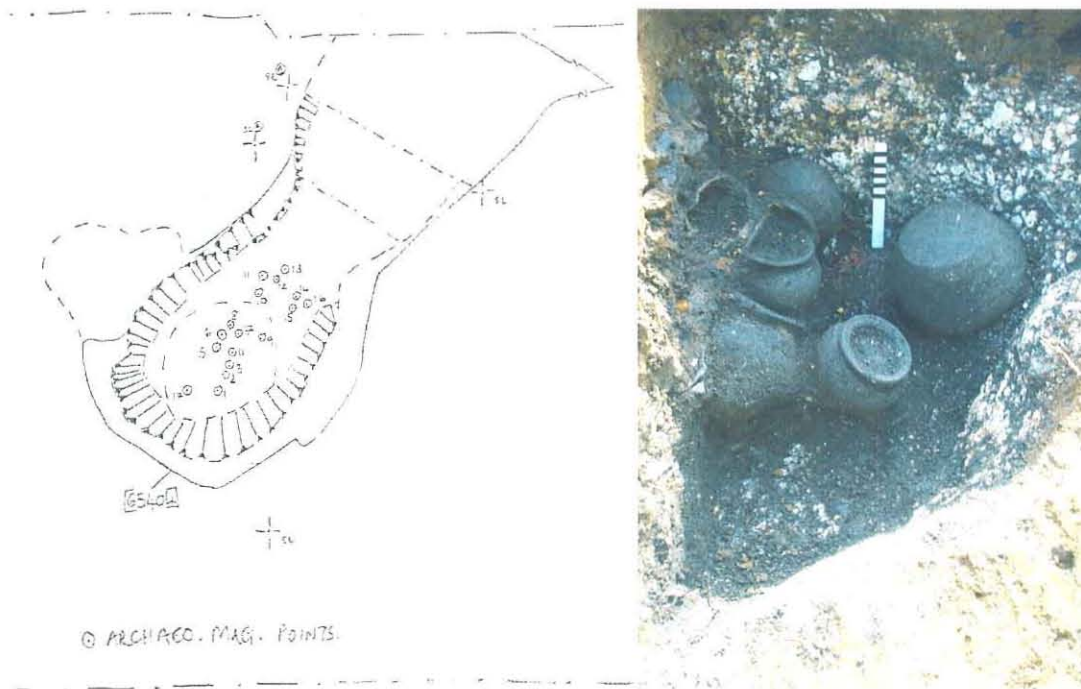


Figure 1; Left: Sketch plan of Michelmersh clamp kiln showing approximate sample locations (not to scale), north is towards the top. Right: Photograph of feature with pots still in-situ, viewed from the west.

Method

Samples were collected using the disc method (see appendix, section 1a) and orientated to true north using a gyro-theodolite. Owing to the steep sides of the kiln it was not possible to obtain a

line of sight to sample 17, so this was orientated to magnetic north using a compass, then corrected to true north using the compass bearing established by the gyro-theodolite. Seventeen samples were collected from the clay floor of the feature and their approximate locations are indicated in the left hand portion of Figure 1. All the samples were composed of black/red, heated clay.

The natural remanent magnetisation (NRM) measured in archaeomagnetic samples is assumed to be caused by thermoremanent magnetisation (TRM) created at the time when the feature of which they were part was last fired. However, a secondary component acquired in later geomagnetic fields can also be present, caused by diagenesis or partial reheating. Additionally, the primary TRM may be overprinted by a viscous component, depending on the grain size distribution within the magnetic material. These secondary components are usually of lower stability than the primary TRM and can thus be removed by partial demagnetisation of the samples.

A typical strategy used in archaeomagnetic analysis of a feature is to first measure the NRM field recorded in the samples. Then each sample is partially demagnetised by exposing it to an alternating magnetic field of fixed peak strength and measuring the resulting changes in its magnetisation. This procedure is repeated with increasing peak field strengths to build up a complete picture of the coercivity spectrum for each sample. The equipment used for these measurements is described in section 2 of the appendix.

After inspection of the coercivity spectrum of each sample, an optimum field strength is selected where it is judged that the maximum amount of secondary magnetisation has been removed, whilst preserving the majority of the primary magnetisation. A mean TRM direction is calculated from the sample measurements made at this optimum partial demagnetisation step. Some samples may be excluded from this calculation if their TRM directions are so anomalous as to make them statistical outliers from the overall TRM distribution. A “magnetic refraction” correction is often applied to the sample mean TRM direction to compensate for distortion of the earth’s magnetic field due to the geometry of the magnetic fabric of the feature itself. Then the mean is adjusted according to the location of the feature relative to a notional central point in the UK (Meriden), so that it can be compared with UK archaeomagnetic calibration data to produce a date of last firing for the feature. Notes concerning the mean calculation and subsequent calibration can be found in sections 3 and 4 of the appendix.

This measurement and calibration strategy was applied to the analysis of the samples from the Michelmersh kiln. As all the samples were taken from the floor of the feature, a magnetic refraction correction of 2.4° was added to the inclinations of the mean TRM direction before calibration.

Results

Sample NRM measurements and measurements after partial demagnetisation are recorded in Table 1. Figure 2 depicts the distribution of the sample TRM directions before and after partial demagnetisation. Tables 2 to 7 record the pilot demagnetisation measurements made on all samples whilst Figures 3-6 graphically illustrate these results for the measurements made on samples 01, 12, 13 and 16 respectively.

The maximum stability of the TRM in each sample was estimated using the method of Tarling and Symons (1967). The maximum stability parameters and ranges over which they persist are listed for each sample in Table 8. In this method, any sample with a maximum stability parameter greater than 2 is judged to record a stable TRM direction. Also listed in Table 8 are a

mean declination and inclination for each sample, calculated from all the partial demagnetisation measurements in its range of maximum stability.

The figures in Table 8 suggest that the magnetisations in samples 01 and 13 were not stable and this is confirmed by visual inspection of the demagnetisation results (Figures 3 and 5 respectively). Sample 14, although apparently stable, has an anomalously shallow inclination in comparison to the other samples. It was taken from an area of the kiln where the surface sloped markedly and it is likely that the sample disk tipped off horizontal whilst the epoxy resin used to attach it was hardening.

These three samples were thus excluded from further analysis. Consideration of the partial demagnetisation results of the remaining 14 samples suggested that a peak field strength of 5mT was necessary to completely remove secondary magnetic components. Figures 4 and 6 illustrate typical demagnetisation behaviour, showing results from sample 12 (most stable) and sample 16 (least stable after rejection of 01, 13 and 14) respectively. Hence the mean TRM vector for the feature was calculated from the measurements made after 5mT partial demagnetisation:

At site: Dec = 23.5° Inc = 67.5° $\alpha_{95} = 1.8^\circ$ k = 486.2
At Meriden: Dec = 24.2° Inc = 68.4°

As confirmation that the correct demagnetisation level had been selected, a second mean was calculated using the mean TRM directions at maximum stability for each sample listed in Table 8. Again samples 01, 13 and 14 were omitted. This mean (Dec = 24.0°, Inc = 67.7°, $\alpha_{95} = 1.85^\circ$, k = 460.7) is statistically almost identical to that quoted above and the test of McFadden and Lowes (1981), indicates a 97% probability that the two are drawn from the same underlying distribution.

Figure 7 shows the comparison of the mean TRM vector with the UK archaeomagnetic calibration curve depicted on a Bauer plot. The date of the last firing of the clamp kiln inferred from it is:

985 AD to 1015 AD at the 63% confidence level.
965 AD to 1030 AD at the 95% confidence level.

Conclusions

Archaeomagnetic study of heated clay samples from the floor of the Michelmersh clamp kiln indicates that they have acquired a TRM owing to the firing of the pots found contained within it. Partial demagnetisation measurements demonstrate that although the stability of the TRM varied between the samples, it was stable up to about 15mT in almost all cases.

Hence it was possible to obtain a mean TRM vector of good precision from the kiln and thus date the last firing of the feature to the end of the 10th century AD. This date agrees well with chronological evidence obtained from pottery typologies. The Michelmersh pottery 'industry' is generally dated to the 11th AD century. However, the earlier part of its chronological range overlaps with the later part of the range of the late Saxon 'sandy wares' which are dated by Biddle and Collis (1978) to 850 to pre 950 AD in Winchester. Overall assessment of the excavated evidence leads Lorraine Mephram, the finds manager at Wessex Archaeology, to expect a date in the mid to later part of 10th century AD for the Michelmersh kiln, in good agreement with the archaeomagnetic evidence.

P. Linford
Archaeometry Branch,
Centre for Archaeology, English Heritage.

Date of report: 15/01/2002

Archaeomagnetic Date Summary

Archaeomagnetic ID:	MM
Feature:	Michelmersh clamp kiln, context 65404
Location:	Longitude 1.5°W, Latitude 51.0°N
Number of Samples (taken/used in mean):	17/14
AF Demagnetisation Applied:	5mT
Distortion Correction Applied:	+2.4°
Declination (at Meriden):	23.5° (24.2°)
Inclination (at Meriden):	67.5° (68.4°)
Alpha-95:	1.8°
k:	486.3
Date range (63% confidence):	985 AD to 1015 AD
Date range (95% confidence):	965 AD to 1030 AD
Independent date estimate:	950 AD to 1050 AD

Sample	Material	NRM Measurements			After Partial Demagnetisation				R
		Dec ^o	Inc ^o	J (mAm ⁻¹)	AF (mT)	Dec ^o	Inc ^o	J (mAm ⁻¹)	
MM01	Clay	32.9	72.6	10.0	5.0	-61.4	15.7	3.5	R
MM02	Clay	35.4	56.5	1083.2	5.0	28.5	61.7	722.6	
MM03	Clay	26.6	68.3	826.6	5.0	26.4	63.1	428.1	
MM04	Clay	22.4	73.8	431.9	5.0	23.3	68.6	236.7	
MM05	Clay	26.1	58.8	402.1	5.0	15.5	60.0	247.3	
MM06	Clay	16.6	67.6	291.5	5.0	18.3	65.5	133.7	
MM07	Clay	21.0	65.1	1293.8	5.0	20.6	63.4	680.9	
MM08	Clay	48.9	66.6	322.4	5.0	31.3	64.8	204.0	
MM09	Clay	34.5	62.8	179.2	5.0	24.6	62.1	115.0	
MM10	Clay	23.4	63.6	775.6	5.0	28.0	63.5	676.8	
MM11	Clay	34.9	66.2	285.7	5.0	23.3	67.8	246.0	
MM12	Clay	22.4	66.0	570.3	5.0	19.0	66.5	438.0	
MM13	Clay	37.6	50.0	229.9	5.0	58.7	49.1	143.8	R
MM14	Clay	-3.2	47.9	404.1	-	-	-	-	R
MM15	Clay	37.9	69.0	1108.5	5.0	32.8	71.6	740.7	
MM16	Clay	41.0	71.9	282.4	5.0	23.5	65.6	102.3	
MM17	Clay	15.2	65.8	222.0	5.0	16.6	66.7	118.9	

Table 1: NRM measurements of samples and measurements after partial AF demagnetisation for feature MM. J = magnitude of magnetisation vector; AF = peak alternating field strength of demagnetising field; R = sample rejected from mean calculation.

AF (mT)	MM01			MM02			MM03		
	Dec ^o	Inc ^o	J (mAm ⁻¹)	Dec ^o	Inc ^o	J (mAm ⁻¹)	Dec ^o	Inc ^o	J (mAm ⁻¹)
0.0	-65.4	62.1	6.7	44.1	65.9	1215.4	32.9	65.1	775.7
1.0	-52.9	54.1	5.7	35.8	64.8	1148.0	-	-	-
2.5	-63.4	45.5	5.0	29.9	62.6	986.5	26.1	63.9	614.2
5.0	-61.4	15.7	3.5	28.5	61.7	722.6	26.4	63.1	428.1
7.5	-67.1	4.9	3.2	29.5	59.5	398.3	27.3	62.1	269.0
10.0	-69.7	-3.2	3.3	27.4	58.7	228.7	28.6	60.3	150.8
15.0	-71.5	-2.3	3.3	23.2	55.8	92.7	32.9	56.5	65.6
20.0	-	-	-	30.4	55.5	50.0	40.1	50.6	40.8

Table 2: Incremental partial demagnetisation measurements for samples MM01, MM02 and MM03.

AF (mT)	MM04			MM05			MM06		
	Dec ^o	Inc ^o	J (mAm ⁻¹)	Dec ^o	Inc ^o	J (mAm ⁻¹)	Dec ^o	Inc ^o	J (mAm ⁻¹)
0.0	32.8	69.5	373.2	24.1	66.4	476.9	4.3	69.8	286.6
1.0	25.9	69.4	362.0	19.9	63.0	418.4	11.9	68.1	252.1
2.5	24.7	69.2	320.8	16.5	61.5	341.7	16.8	66.5	202.2
5.0	23.3	68.6	236.7	15.5	60.0	247.3	18.3	65.5	133.7
7.5	25.1	67.5	150.5	19.4	56.5	137.8	18.5	64.2	80.8
10.0	22.6	67.2	96.1	18.3	54.4	88.2	16.1	64.2	52.1
15.0	19.8	63.8	42.0	23.6	45.5	30.3	12.0	58.1	25.2
20.0	17.4	54.3	21.6	11.7	21.0	23.0	-0.8	50.5	14.8

Table 3: Incremental partial demagnetisation measurements for samples MM04, MM05 and MM06.

AF (mT)	MM07			MM08			MM09		
	Dec ^o	Inc ^o	J (mAm ⁻¹)	Dec ^o	Inc ^o	J (mAm ⁻¹)	Dec ^o	Inc ^o	J (mAm ⁻¹)
0.0	18.8	71.3	1169.1	37.0	61.1	359.2	21.5	64.4	171.5
1.0	19.3	67.5	1097.4	33.2	62.6	325.2	23.4	63.1	162.4
2.5	20.6	65.2	969.4	32.6	63.8	280.0	24.5	62.3	146.0
5.0	20.6	63.4	680.9	31.3	64.8	204.0	24.6	62.1	115.0
7.5	21.7	62.8	417.6	35.9	66.2	127.7	22.8	61.6	83.6
10.0	21.2	62.3	276.9	37.0	65.0	92.4	19.3	61.0	63.6
15.0	28.8	62.1	94.7	47.7	66.2	46.8	5.0	59.0	31.4
20.0	22.0	59.4	49.9	45.7	59.5	29.2	-10.8	51.4	16.1
30.0	-	-	-	-	-	-	-34.9	31.9	8.3

Table 4: Incremental partial demagnetisation measurements for samples MM07, MM08 and MM09.

AF (mT)	MM10			MM11			MM12		
	Dec ^o	Inc ^o	J (mAm ⁻¹)	Dec ^o	Inc ^o	J (mAm ⁻¹)	Dec ^o	Inc ^o	J (mAm ⁻¹)
0.0	23.6	64.9	855.0	22.3	67.4	299.4	22.6	66.8	561.5
1.0	25.7	63.9	820.7	24.1	67.3	288.5	20.9	66.8	536.5
2.5	26.9	63.6	766.6	22.5	67.5	270.0	20.4	66.6	495.6
5.0	28.0	63.5	676.8	23.3	67.8	246.0	19.0	66.5	438.0
7.5	28.7	63.8	598.6	24.4	67.3	219.3	19.7	67.0	387.1
10.0	27.0	63.7	530.3	24.3	66.9	197.0	18.9	67.1	341.6
15.0	28.2	62.3	356.9	23.9	65.5	139.9	17.8	66.6	248.7
20.0	25.8	61.8	196.7	22.9	63.7	79.9	17.3	66.6	165.0
30.0	21.7	58.8	73.2	7.1	61.3	31.1	12.2	65.3	74.2
40.0	17.0	54.4	43.1	4.5	55.9	16.5	6.5	61.1	39.5

Table 5: Incremental partial demagnetisation measurements for samples MM10, MM11 and MM12.

AF (mT)	MM13			MM14			MM15		
	Dec ^o	Inc ^o	J (mAm ⁻¹)	Dec ^o	Inc ^o	J (mAm ⁻¹)	Dec ^o	Inc ^o	J (mAm ⁻¹)
0.0	54.2	60.6	288.3	10.0	55.0	430.0	34.5	73.8	1079.2
1.0	51.6	58.2	252.4	7.6	52.3	411.4	31.6	71.6	1012.2
2.5	52.4	54.8	207.9	7.5	51.2	395.6	30.9	71.2	920.9
5.0	58.7	49.1	143.8	-	-	-	32.8	71.6	740.7
7.5	66.3	37.8	95.5	5.3	45.8	307.4	34.7	72.1	591.4
10.0	70.4	22.4	68.0	5.4	44.1	271.6	37.4	71.8	474.9
15.0	68.6	-27.3	47.4	3.2	39.7	205.7	34.5	70.3	248.3
20.0	51.1	-59.8	54.8	1.0	36.4	132.6	29.7	69.3	143.9
30.0	-	-	-	-1.9	25.6	59.8	23.3	66.8	69.2
40.0	-	-	-	-9.1	18.0	35.6	-	-	-

Table 6: Incremental partial demagnetisation measurements for samples MM13, MM14 and MM15.

AF (mT)	MM16			MM17		
	Dec ^o	Inc ^o	J (mAm ⁻¹)	Dec ^o	Inc ^o	J (mAm ⁻¹)
0.0	35.3	75.9	254.6	25.0	74.4	280.6
1.0	26.3	70.2	227.7	20.7	69.6	236.9
2.5	25.4	67.3	174.1	19.1	67.7	188.4
5.0	23.5	65.6	102.3	16.6	66.7	118.9
7.5	20.2	62.4	55.3	15.3	67.1	75.3
10.0	11.6	60.5	32.2	8.6	68.7	50.5
15.0	1.6	43.7	14.7	1.2	65.1	28.3
20.0	2.3	47.9	6.4	-11.8	73.9	22.5

Table 7: Incremental partial demagnetisation measurements for samples MM16 and MM17.

Sample	Range min. (mT)	Range max. (mT)	Max. Stability	Dec ^o	Inc ^o
MM01	7.5	15.0	1.7	-69.4	-0.2
MM02	2.5	10.0	4.5	28.8	60.6
MM03	2.5	7.5	7.5	26.6	63
MM04	1.0	5.0	10.1	24.6	69.1
MM05	1.0	5.0	3.4	17.2	61.5
MM06	5.0	10.0	7.5	17.6	64.6
MM07	5.0	10.0	11.7	21.2	62.8
MM08	2.5	10.0	5.8	34.2	65
MM09	2.5	7.5	11.8	24	62
MM10	2.5	10.0	21.6	27.6	63.7
MM11	0.0	10.0	21.6	23.5	67.4
MM12	5.0	20.0	26.1	18.5	66.8
MM13	0.0	2.5	1.7	52.7	57.9
MM14	7.5	15.0	2.6	4.6	43.2
MM15	1.0	5.0	16.5	31.8	71.5
MM16	1.0	5.0	2.6	25	67.7
MM17	2.5	7.5	7.9	17	67.2

Table 8: Assessment of the range of demagnetisation values over which each sample attained its maximum directional stability using the method of Tarling and Symons (1967). The declination and inclination values quoted are for the mean TRM direction for the sample calculated for all demagnetisation measurements in its range of maximum stability.

Appendix: Standard Procedures for Sampling and Measurement

1) Sampling

One of three sampling techniques is employed depending on the consistency of the material (Clark, Tarling and Noel 1988):

- a) **Consolidated materials:** Rock and fired clay samples are collected by the disc method. Several small levelled plastic discs are glued to the feature, marked with an orientation line related to True North, then removed with a small piece of the material attached.
- b) **Unconsolidated materials:** Sediments are collected by the tube method. Small pillars of the material are carved out from a prepared platform, then encapsulated in levelled plastic tubes using plaster of Paris. The orientation line is then marked on top of the plaster.
- c) **Plastic materials:** Waterlogged clays and muds are sampled in a similar manner to method 1b) above; however, the levelled plastic tubes are pressed directly into the material to be sampled.

2) Physical Analysis

- a) Magnetic remanences are measured using a slow speed spinner fluxgate magnetometer (Molyneux et al. 1972; see also Tarling 1983, p84; Thompson and Oldfield 1986, p52).
- b) Partial demagnetisation is achieved using the alternating magnetic field method (As 1967; Creer 1959; see also Tarling 1983, p91; Thompson and Oldfield 1986, p59), to remove viscous magnetic components if necessary. Demagnetising fields are measured in milli-Tesla (mT), figures quoted being for the peak value of the field.

3) Remanent Field Direction

- a) The remanent field direction of a sample is expressed as two angles, declination (Dec) and inclination (Inc), both quoted in degrees. Declination represents the bearing of the field relative to true north, angles to the east being positive; inclination represents the angle of dip of this field.
- b) Aitken and Hawley (1971) have shown that the angle of inclination in measured samples is likely to be distorted owing to magnetic refraction. The phenomenon is not well understood but is known to depend on the position the samples occupied within the structure. The corrections recommended by Aitken and Hawley are applied, where appropriate, to measured inclinations, in keeping with the practise of Clark, Tarling and Noel (1988).
- c) Individual remanent field directions are combined to produce the mean remanent field direction using the statistical method developed by R. A. Fisher (1953). The quantity α_{95} , "alpha-95", is quoted with mean field directions and is a measure of the precision of the determination (see Aitken 1990, p247). It is analogous to the

standard error statistic for scalar quantities; hence the smaller its value, the better the precision of the date.

- d)** For the purposes of comparison with standardised UK calibration data, remanent field directions are adjusted to the values they would have had if the feature had been located at Meriden, a standard reference point. The adjustment is done using the method suggested by Noel (Tarling 1983, p116).

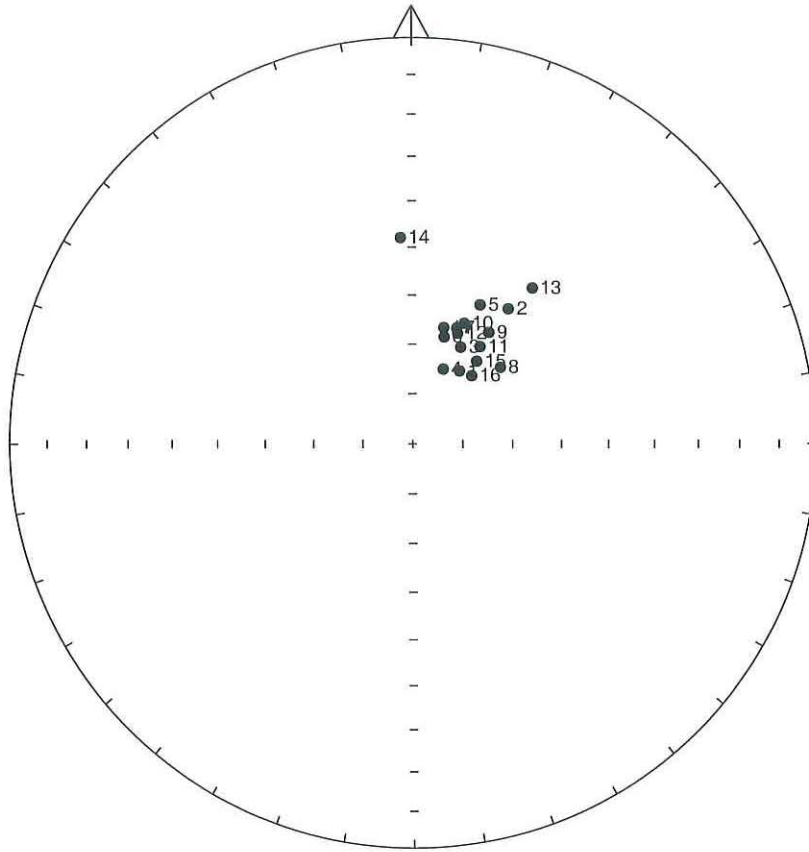
4) Calibration

- a)** Material less than 3000 years old is dated using the archaeomagnetic calibration curve compiled by Clark, Tarling and Noel (1988).
- b)** Older material is dated using the lake sediment data compiled by Turner and Thompson (1982).
- c)** Dates are normally given at the 63% and 95% confidence levels. However, the quality of the measurement and the estimated reliability of the calibration curve for the period in question are not taken into account, so this figure is only approximate. Owing to crossovers and contiguities in the curve, alternative dates are sometimes given. It may be possible to select the correct alternative using independent dating evidence.
- d)** As the thermoremanent effect is reset at each heating, all dates for fired material refer to the final heating.
- e)** Dates are prefixed by "cal", for consistency with the new convention for calibrated radiocarbon dates (Mook 1986).

References

- Aitken, M. J. 1990. *Science-based Dating in Archaeology*. London: Longman.
- Aitken, M. J. and H. N. Hawley 1971. Archaeomagnetism: evidence for magnetic refraction in kiln structures. *Archaeometry* **13**, 83-85.
- As, J. A. 1967. The a.c. demagnetisation technique, in *Methods in Palaeomagnetism*, D. W. Collinson, K. M. Creer and S. K. Runcorn (eds). Amsterdam: Elsevier.
- Biddle M., and Collis J., 1978. A new type of 9th and 10th century pottery from Winchester. *Medieval Archaeology* **22**, 133-135.
- Clark, A. J., D. H. Tarling and M. Noel 1988. Developments in Archaeomagnetic Dating in Britain. *J. Arch. Sci.* **15**, 645-667.
- Creer, K. M. 1959. A.C. demagnetisation of unstable Triassic Keuper Marls from S. W. England. *Geophys. J. R. Astr. Soc.* **2**, 261-275.
- Fisher, R. A. 1953. Dispersion on a sphere. *Proc. R. Soc. London A* **217**, 295-305.
- McFadden, P. L. and Lowes, F. J. 1981. The discrimination of mean directions drawn from Fisher distributions. *Geophys. J. R. astr. Soc.* **67**, 53-58.
- Molyneux, L., R. Thompson, F. Oldfield and M. E. McCallan 1972. Rapid measurement of the remanent magnetisation of long cores of sediment. *Nature* **237**, 42-43.
- Mook, W. G. 1986. Recommendations/Resolutions Adopted by the Twelfth International Radiocarbon Conference. *Radiocarbon* **28**, M. Stuiver and S. Kra (eds), 799.
- Tarling, D. H. 1983. *Palaeomagnetism*. London: Chapman and Hall.
- Tarling, D. H. and Symons, D. T. A. 1967. A stability index of remanence in palaeomagnetism. *Geophys. J. R. astr. Soc.* **12**, 443-448.
- Thompson, R. and F. Oldfield 1986. *Environmental Magnetism*. London: Allen and Unwin.
- Turner, G. M. and R. Thompson 1982. Detransformation of the British geomagnetic secular variation record for Holocene times. *Geophys. J. R. Astr. Soc.* **70**, 789-792.

a)



b)

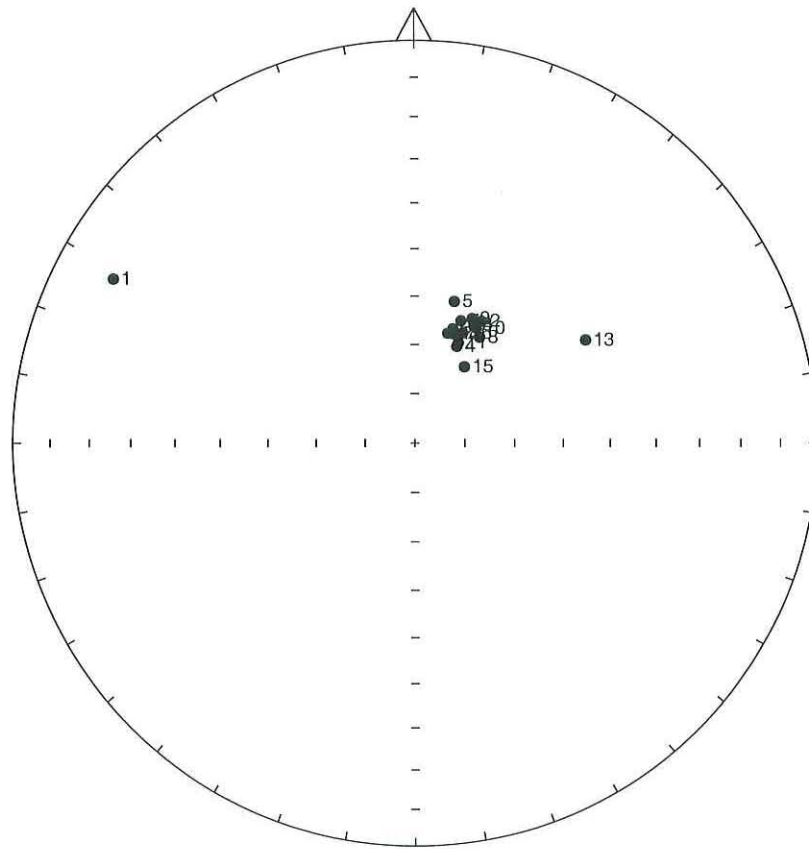
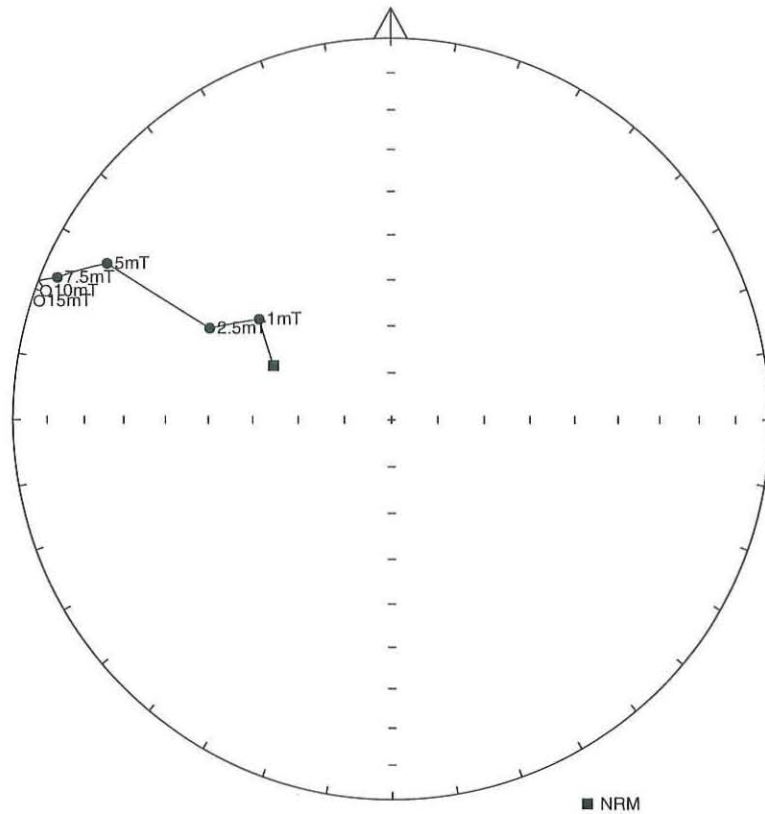


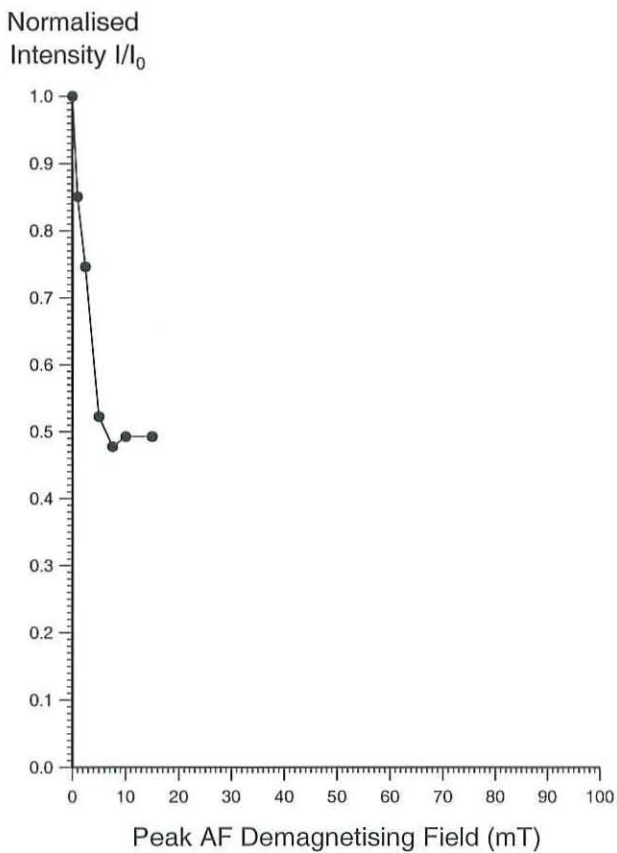
Figure 2: a) Distribution of NRM directions of samples from feature MM represented as an equal area stereogram. In this projection declination increases clockwise with zero being at 12 o'clock while inclination increases from zero at the equator to 90 degrees in the centre of the projection. Open circles represent negative inclinations. b) Distribution of thermoremanent directions of magnetisation of the same samples after partial AF demagnetisation to 5mT.

a)



■ NRM

b)



c)

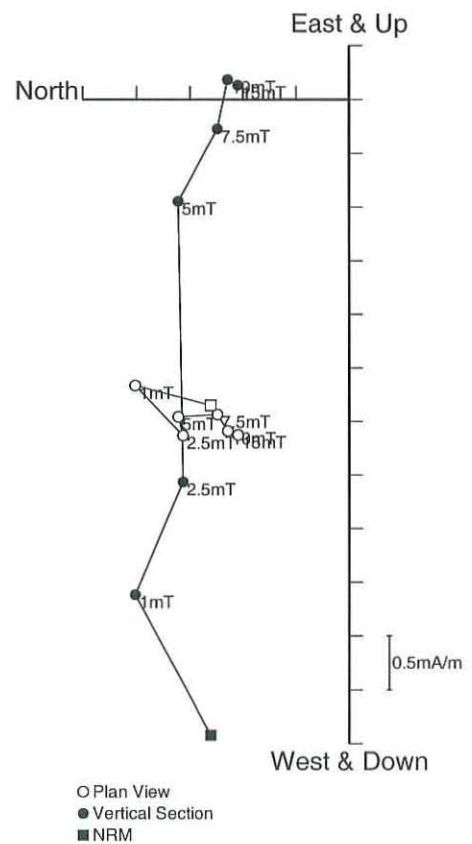
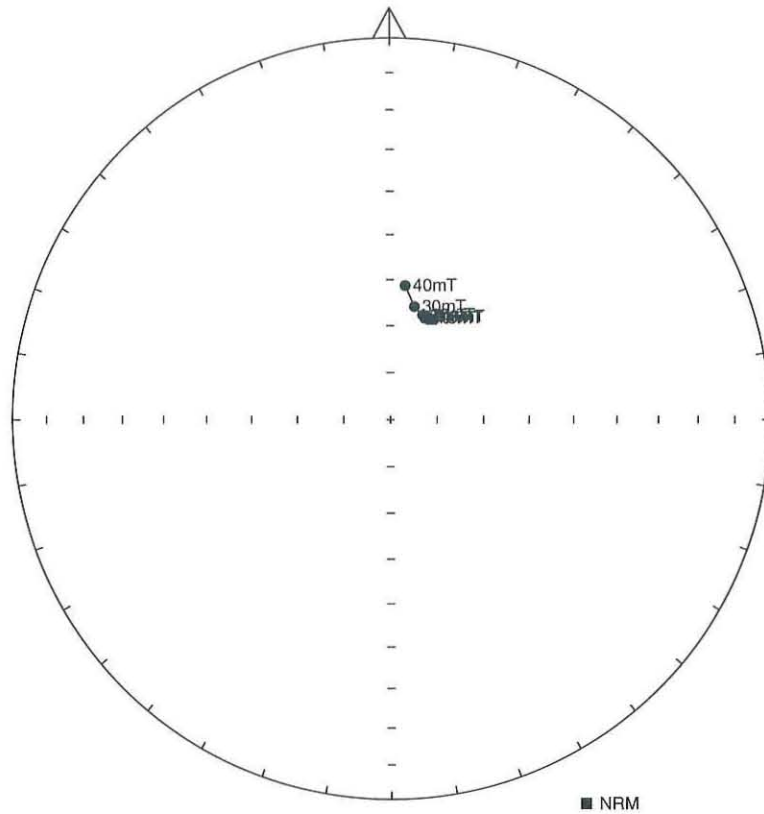
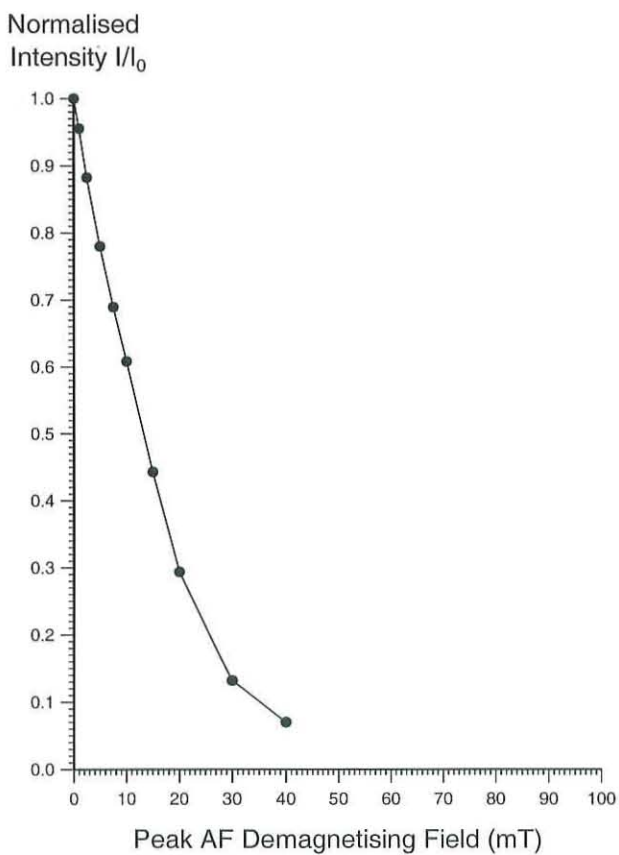


Figure 3: Stepwise AF demagnetisation of sample MM01. Diagram a) depicts the variation of the remanent direction as an equal area stereogram (declination increases clockwise, while inclination increases from zero at the equator to 90 degrees at the centre of the projection); b) shows the normalised change in remanence intensity as a function of the demagnetising field; c) shows the changes in both direction and intensity as a vector endpoint projection.

a)



b)



c)

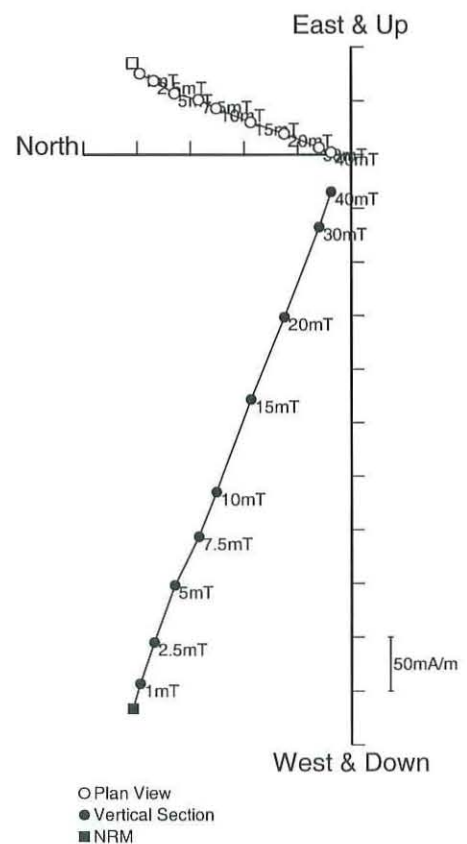
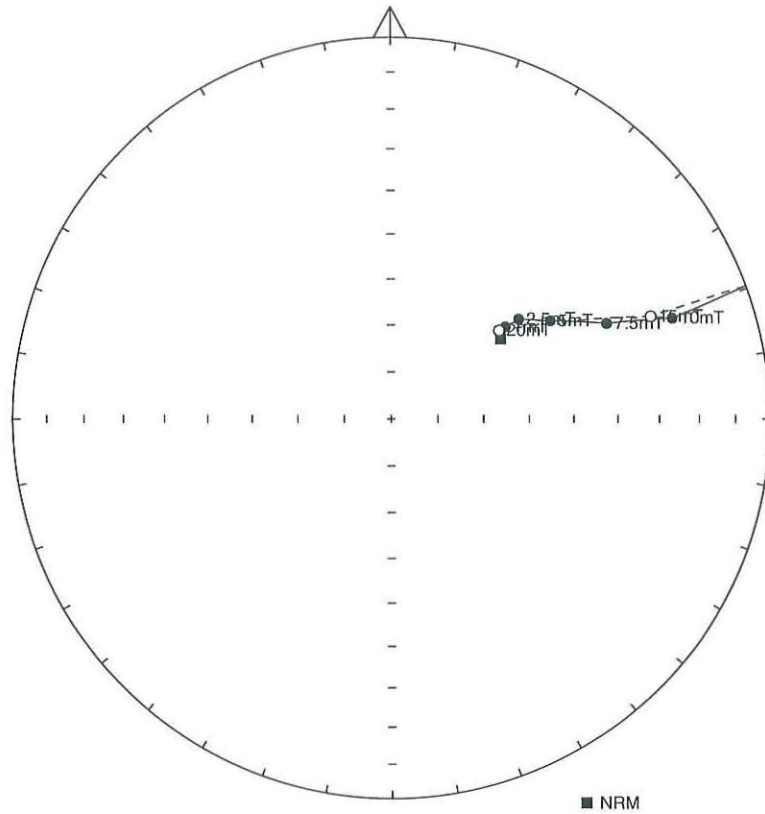
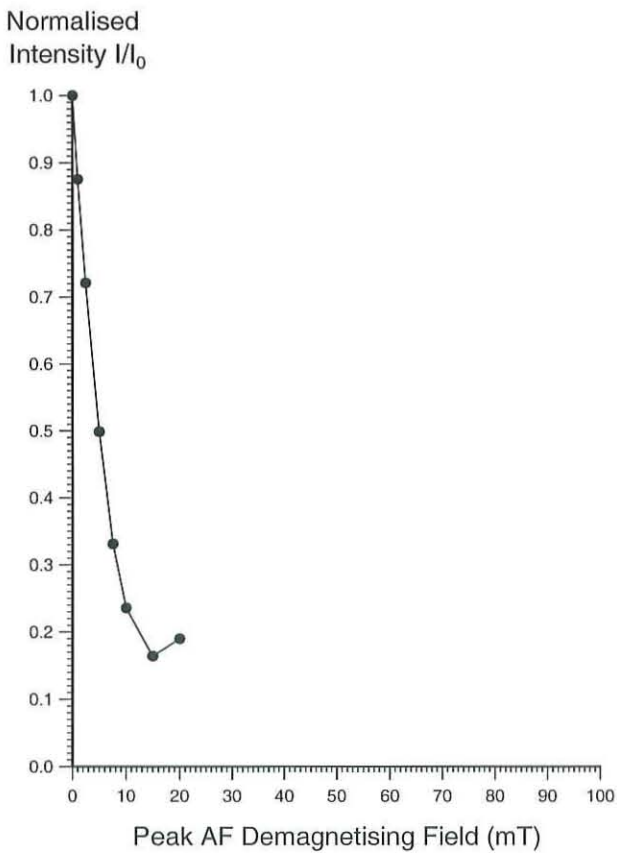


Figure 4: Stepwise AF demagnetisation of sample MM12. Diagram a) depicts the variation of the remanent direction as an equal area stereogram (declination increases clockwise, while inclination increases from zero at the equator to 90 degrees at the centre of the projection); b) shows the normalised change in remanence intensity as a function of the demagnetising field; c) shows the changes in both direction and intensity as a vector endpoint projection.

a)



b)



c)

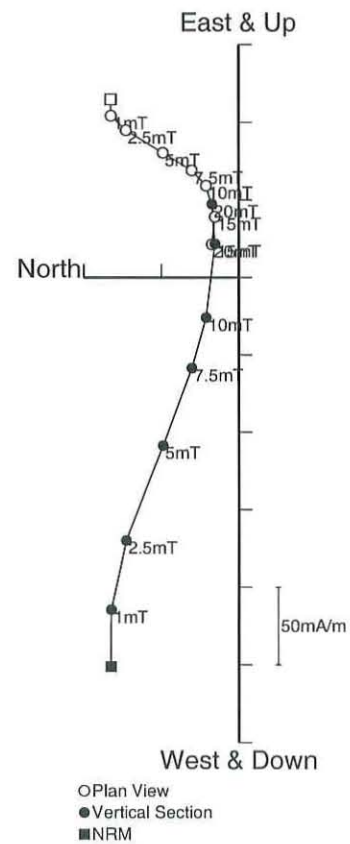
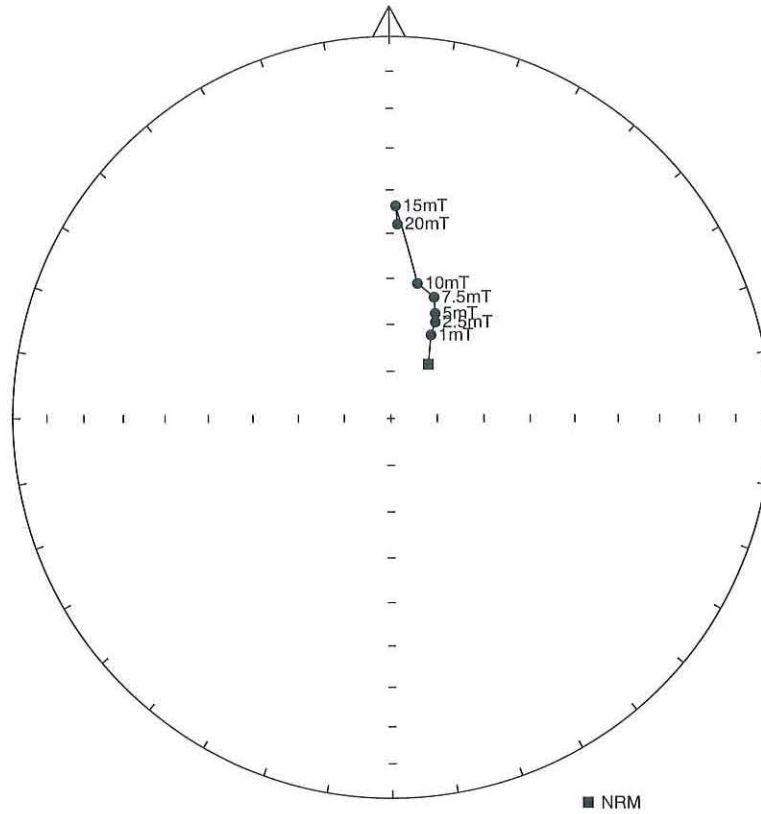
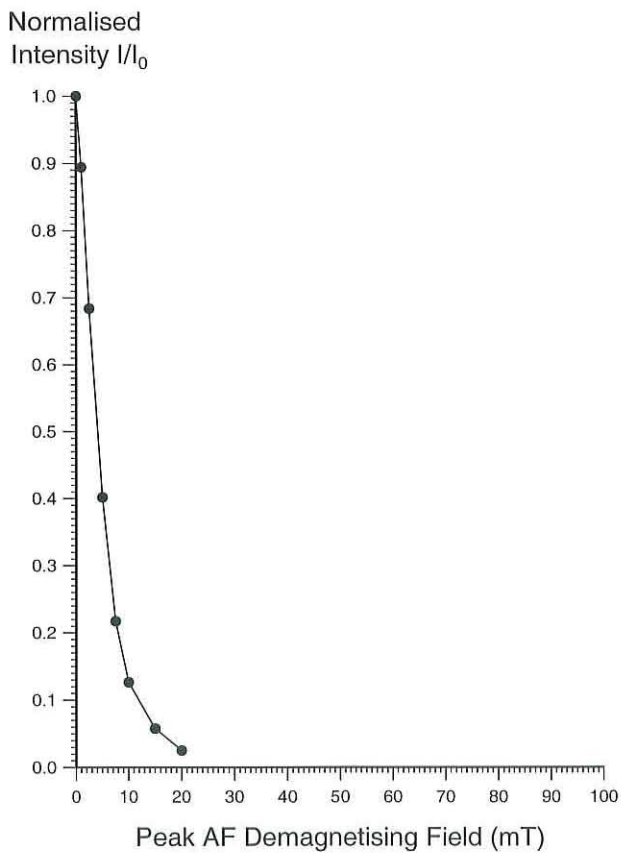


Figure 5: Stepwise AF demagnetisation of sample MM13. Diagram a) depicts the variation of the remanent direction as an equal area stereogram (declination increases clockwise, while inclination increases from zero at the equator to 90 degrees at the centre of the projection); b) shows the normalised change in remanence intensity as a function of the demagnetising field; c) shows the changes in both direction and intensity as a vector endpoint projection.

a)



b)



c)

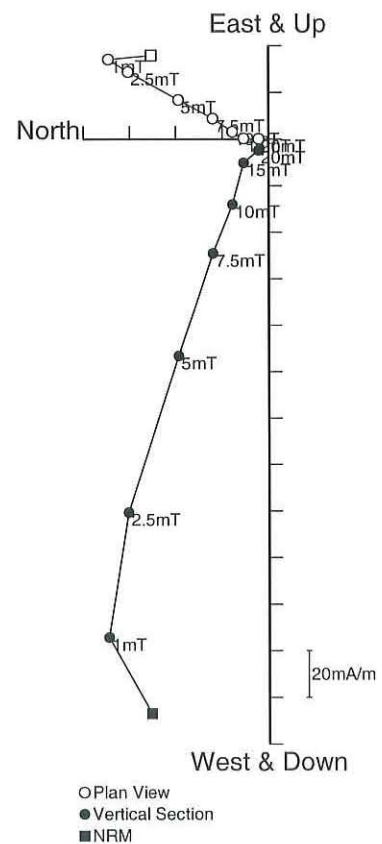


Figure 6: Stepwise AF demagnetisation of sample MM16. Diagram a) depicts the variation of the remanent direction as an equal area stereogram (declination increases clockwise, while inclination increases from zero at the equator to 90 degrees at the centre of the projection); b) shows the normalised change in remanence intensity as a function of the demagnetising field; c) shows the changes in both direction and intensity as a vector endpoint projection.

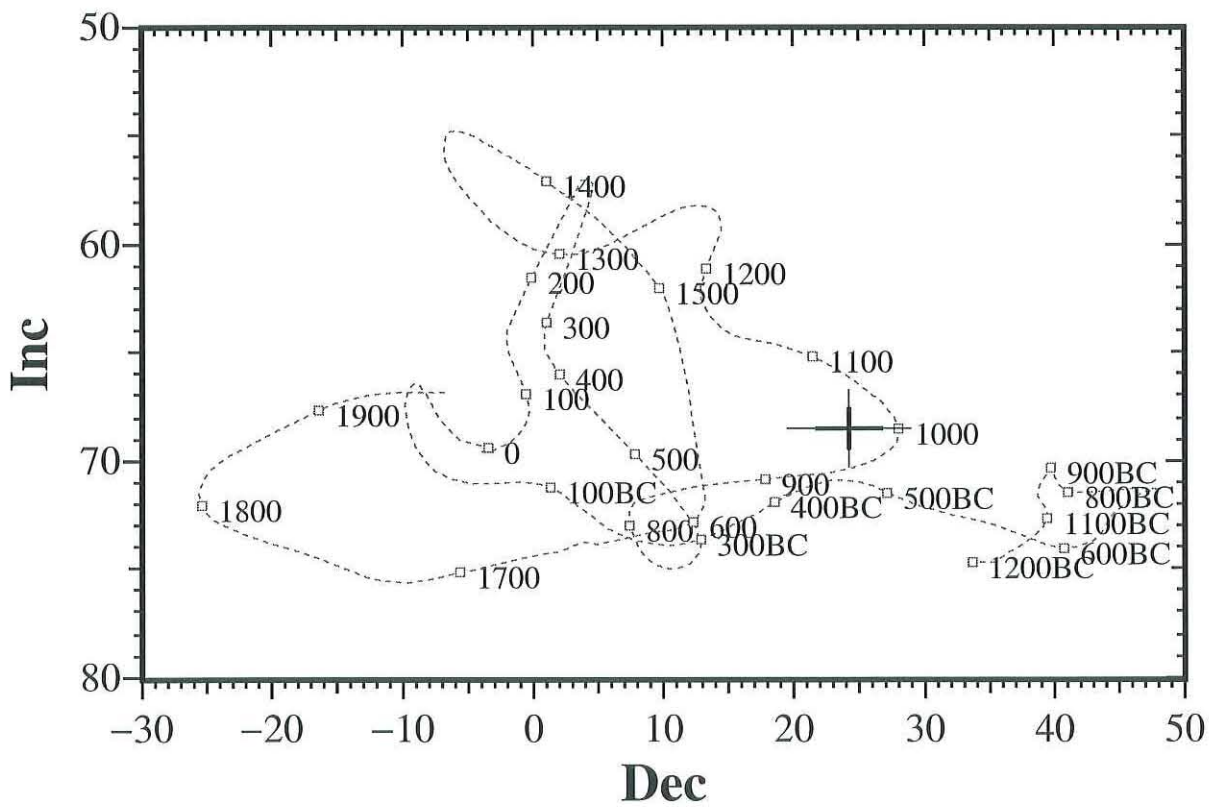


Figure 7: Comparison of the mean thermoremanent vector calculated from samples 02-12 and 15-17 from feature MM after 5mT partial demagnetisation with the UK master calibration curve. Thick error bar lines represent 63% confidence limits and narrow lines 95% confidence limits.